Numerical comparison of different solution methods for optimal boundary control problems in thermal fluid dynamics

Daniele Cerroni, Sandro Manservisi and Filippo Menghini

***Abstract*—**In this paper we propose and compare different methods for the solution of the control-adjoint-state optimality system which minimizes an objective functional in temperature. The minimization is constrained by the energy convection-diffusion equation with velocity field defined by the incompressible Navier-Stokes system. Three methods, based on different solution spaces, for solving the adjoint-state optimality system are compared. In the first one, as in the standard approach, the controlled temperature field is assumed to belong to a regular class of solutions with smooth derivatives and the resulting control-adjoint-state optimality system is solved in a segregated way. In the second one we introduce a fully coupled solution approach, where, in order to obtain a more robust numerical algorithm, the boundary control is extended to the interior and Dirichlet conditions are implicitly enforced through a volumetric force term. In the last approach we introduce Discontinuous Galerkin formulation for the energy equation in order to seek discontinuous solutions. Numerical two and three-dimensional test cases are reported in order to show the validity of the proposed approaches. The results are compared in term of solution smoothness and achievement of low values of the objective functional.

***Keywords*—**Optimal Boundary Control, Temperature Control.

I. Introduction

In recent years the optimal control of temperature distribution in fluid dynamics problems has gained popularity because of many engineering applications in heat transfer and industrial processes. However the numerical computation of the optimal solution is a rather CPU time consuming task and the development of robust and stable numerical tools for such optimization problems is still an open challenge.

In optimal control theory different types of controls, such as distributed, boundary and shape controls are considered, see for a review [1]-[2]. In particular, in the first one, source terms are used as control parameters to simulate heat generation. For convection-diffusion problems like the energy equation the interested reader can see [3]-[6]. For numerical treatments of the optimal control of Navier-Stokes or MHD equations one can consult [7]-[9], while for Boussinesq and MHD equations [10]-[11]. Due to practical issues it is difficult to set control devices inside the system and this type of control cannot often be applied. In such cases the boundary control may be a possible approach. This type of control can be implemented in a very simple way by injecting fluid with different properties or setting temperature on the wall. However, boundary control is more challenging than the distributed one, from the theoretical point of view and in the construction of feasible computational algorithms. For an application to the Navier-Stokes boundary optimal control see for example [12] and citations therein. In shape control the geometrical properties of the system can be changed in order to obtain the desired result. A common application of this type of control is airplane or car wing design [8]. Other techniques are available for control problems, like linear feedback methods. In [13]-[15], examples of this technique applied to the Boussinesq, Navier-Stokes and energy equations are studied.

The most challenging task arising in the study of optimal control problems and particularly in boundary control is the numerical solution of the optimality system. The solution of the control-adjoint-state optimality system can be obtained in different ways. The equations can be solved separately in a segregated way or the whole system can be solved in a fully coupled way. The coupled implicit solution of the state, adjoint and control equations is robust while in the segregated case oscillations may appear. When the system is non-linear the segregated solution can be a natural choice, however the penalty parameters in the regularization terms of the objective functional are limited by numerical errors. In fact if these parameters tends to zero the solution loses smoothness and the numerical algorithm may not converge.

In this paper we consider an optimal boundary control problem for temperature and Navier-Stokes equations. Heat convection is regarded as the dominant physical mechanism for heat transfer and the effects of temperature on velocity and pressure, such as buoyancy, are neglected. We consider a boundary optimal control problem for the temperature equation where the control is performed through the boundary conditions of temperature on well-defined parts of the boundary and the objective functional is given in the following form

Filippo Menghini is with the Department of Industrial Engineering, University of Bologna, via dei Colli 16, 40136 Bologna Italy. (Tel: +39 0512087722; e-mail: filippo.menghini3@unibo.it).

Daniele Cerroni and Sandro Manservisi are with the Department of Industrial Engineering, University of Bologna, via dei Colli 16, 40136 Bologna Italy.

$$J(T,g) = \frac{1}{2}\int_\Omega (T(x)-T_d)^2 w(x)d\Omega + \frac{\beta}{2}\int_{\Gamma_c} \|g\|^2\, d\Gamma + \\ + \frac{\lambda}{2}\int_{\Gamma_c} \|\nabla g\|^2 d\Gamma \quad (1)$$

where T(x) is the temperature distribution, T_d is the desired temperature, w(x) is a weight function that can be used to improve the control, Γ_c is the surface on which the control is imposed and g is the controlled temperature. This functional consists of three terms: the objective and two regularization terms. The two parameters β and λ can be used to impose a more smooth controlled temperature. In particular if both parameters are different from zero the function g is differentiable while for vanishing λ we have only square integrability. We consider and analyze three cases. In the first case we set λ = 0 and use standard Lagrangian quadratic elements. Since g is the trace of the gradient of the adjoint variable it is not possible to evaluate directly its numerical values, so we rewrite the boundary control equation in a volumetric form. In the second case we still set λ = 0 and use discontinuous Galerkin method [16]-[17]. In the first two approaches we solve the optimality system with a fully coupled one-shot algorithm, which is very efficient and fast. In the third case we consider the full functional and find a solution in more regular spaces. We solve this optimality system in a segregated way with standard quadratic elements for all state-adjoint variables.

The paper is organized as follows: in the next section we describe the optimality system and the solution strategies. In the subsequent section we report the numerical results of two and three-dimensional test cases obtained by implementing the three solution approaches. A comparison between the solutions is carried on and different features of the three approaches are highlighted. Finally in the last section we draw our conclusion.

II. Optimality System

Let Ω be an open set with boundary Γ. The optimality system on Ω can be obtained by minimizing the objective functional under the constraints imposed by the energy equation and the Navier-Stokes system. The Navier-Stokes equations for an incompressible flow are

$$\nabla \cdot v = 0 \quad (2)$$

$$\rho\,(v\cdot\nabla)v = -\nabla p + \mu\,\nabla^2 v \quad (3)$$

where μ is the dynamical viscosity, ρ the density and p the pressure. The steady state energy equation together with the boundary conditions can be written as

$$(v\cdot\nabla)T = \alpha\,\nabla^2 T \quad (4)$$

$$\frac{\partial T}{\partial n} = d \quad on\ \Gamma_n$$

$$T = g \quad on\ \Gamma_c$$

where v is the fluid velocity and α is the fluid thermal diffusivity. We assume that the value of the heat flux d is given. The optimal control problem consists in finding the best possible g in order to minimize the functional (1).

Let us recall some notations about functional spaces used in the rest of the paper. We will use the standard notation for the Sobolev spaces $H^s(\Omega)$ with norm $\|\ \|_s$ ($H^0(\Omega)= L^2(\Omega)$ and $\|\ \|_0=\|\ \|$). Let $H^s_0(\Omega)$ be the closure of $C^\infty_0(\Omega)$ under the norm $\|\ \|_s$ and $H^{-s}(\Omega)$ be the dual space of $H^s_0(\Omega)$. The trace space for the functions in $H^1(\Omega)$ will be denoted by $H^{1/2}(\Gamma)$. For details on these spaces, one can consult [18]-[19].

By writing the total Lagrangian and setting its Fréchet derivatives to zero we can obtain the weak form of the optimality system [7]-[11]

$$\int_\Omega [(v\cdot\nabla)T]\phi\, d\Omega + \int_\Omega \alpha\,\nabla T\cdot\nabla\phi\, d\Omega \\ - \int_{\Gamma_n} \alpha\,\nabla T\cdot n\,\phi\, d\Gamma = 0, \qquad \forall\,\phi\ \in H^1(\Omega) \quad (5)$$

$$\int_\Omega \theta[(v\cdot\nabla)\psi]\, d\Omega + \int_\Omega \alpha\,\nabla\theta\cdot\nabla\psi\, d\Omega \\ - \int_{\Gamma_n} \alpha\,\nabla\theta\cdot n\,\psi\, d\Gamma \\ = \int_\Omega (T-T_d)\psi\, d\Omega, \qquad \forall\,\psi\ \in H^1(\Omega) \quad (6)$$

$$\int_{\Gamma_c} \beta g\chi\, d\Gamma + \int_{\Gamma_c} \lambda\,\nabla g\cdot\nabla\chi\, d\Gamma \\ = \int_{\Gamma_c} \alpha\,\nabla\theta\cdot n\,\chi\, d\Gamma, \qquad \forall\ \chi\ \in H^{1/2}(\Gamma_c) \quad (7)$$

The adjoint temperature θ is the Lagrange multiplier satisfying (6). The (7), defined only on the controlled surface, is the equation for the control temperature g. The functions $\chi \in H^{1/2}(\Gamma_c)$ are the restrictions of the test functions $\psi \in H^1(\Omega)$ over Γ_c. If one approximates the above spaces with the finite dimensional ones the finite element approximation is obtained.

The fluid velocity in the state and adjoint equations (5-6) is computed by solving the Navier-Stokes system. In order to introduce these equations, we set

$$a(v,u) = \int_\Omega \nabla v{:}\,\nabla u\ d\Omega \quad (8)$$

$$d(u,q) = \int_\Omega q\,\nabla\cdot u\ d\Omega \quad (9)$$

$$c(v,u,\omega) = \int_\Omega (v\cdot\nabla)u\cdot\omega\, d\Omega \quad (10)$$

for all u, v, $\omega \in H^1(\Omega)$ and $q \in L^2_0(\Omega)$ with the Reynolds number defined as

$$Re = \frac{\rho\, U\, L}{\mu}, \quad (11)$$

where ρ, U, L, μ denote the reference values for density, velocity, length and dynamic viscosity, respectively. Given $v_0 \in H^{1/2}(\Gamma)$, we seek $(v, p, \tau) \in H^1(\Omega) \times L^2_0(\Omega) \times H^{-1}(\Omega)$ such

that

$$\frac{1}{Re}a(v,u) + c(v,v,u) + d(u,p) + (\tau,u) = 0 \quad \forall u \in H^1(\Omega) \tag{12}$$

$$d(v,q) = 0 \quad \forall q \in L_0^2(\Omega) \tag{13}$$

where v=v_0 on Γ and τ is the stress boundary vector [7]-[12]-[14]. The velocity field is computed from the Navier-Stokes equations (12-13) before solving the optimality system since we do not consider temperature dependent properties of the fluid.

We now describe and compare three different approaches for the solution of the system (5-7). In the first case we set the parameter λ=0 so we seek a solution for the controlled temperature in $L_0^2(\Omega)$. In this case the (7) can be solved by

$$T = g = \alpha \frac{\nabla\theta \cdot n}{\beta} \; on \; \Gamma_c \tag{14}$$

In order to evaluate T from θ on Γ_c we can proceed in the following way

$$\int_{\Gamma_c} \beta T \chi \, d\Gamma = \int_{\Gamma_c} \alpha \, \nabla\theta \cdot n \, \chi \, d\Gamma, \quad \forall \chi \in H^{\frac{1}{2}}(\Gamma_c) \tag{15}$$

which can be rewritten, using equation (6), as

$$\int_{\Gamma_c} \beta T \psi \, d\Gamma = \int_{\Omega} \theta[(v \cdot \nabla)\psi] \, d\Omega + \int_{\Omega} \alpha \, \nabla\theta \cdot \nabla\psi \, d\Omega - \int_{\Omega} (T - T_d)\psi \, d\Omega, \quad \forall \psi \in H^1(\Omega) \tag{16}$$

where the test function χ is the restriction of ψ on Γ_c. We remark that the temperature control (14) is the trace of the function $\nabla\theta \in L^2(\Omega)$ which is difficult to evaluate numerically. The expression (16) allows an easy computation of T=g on the boundary since all the right hand side functions are well defined on Ω.

In the second case we still assume λ=0 and use the Discontinuous Galerkin method for the solution of the energy equation. Therefore we impose Dirichlet boundary conditions by setting T=g on Γ_c. The use of Discontinuous Galerkin is appropriate for this setting since we have $\beta \neq 0$ and the solution $g \in L^2(\Gamma_c)$. We remark that $\beta = 0$ implies $g \in H^{1/2}(\Gamma_c)$, [9]-[10]-[12]. In the first two cases we solve the optimality system with a one-shot solver because the system is linear and the control g is computed implicitly.

In the third case we assume $\lambda \neq 0$ which implies $g \in H^1(\Gamma_c)$. In this case the differential equation (7) must be solved on the boundary. Extra boundary conditions over $\partial\,\Gamma_c$ must be enforced. We solve this optimality system in a segregated way with standard quadratic elements for all the three variables T, θ and g. Since we cannot use a one-shot solver because the equations are segregated, the following algorithm could be used to obtain the final solution:

1. assign an initial condition for the temperature on the controlled boundary g^i;
2. solve energy equation (5) with the control g^i;
3. solve adjoint energy equation (6) with temperature computed at the previous step;
4. solve control equation (7) with adjoint temperature computed at the previous step to obtain the new g^{i+1};
5. start again from step 2 setting i=i+1 until convergence is reached ($g^{i+1} \approx g^i$).

We have found however that this algorithm does not converge monotonically and often convergence is not reached. One may introduce the following changes to the algorithm to obtain a more stable solution process:

1) assign an initial condition for the temperature on the controlled boundary g^i;
2) solve energy equation (5) with the control g^i;
3) solve adjoint energy equation (6) with temperature computed at the previous step;
4) solve control equation (7) with adjoint temperature computed at the previous step to obtain the new g^{i+1};
   a) compute the functional J(T,g) in (1) and assign an initial η;
   b) solve energy equation (5) with the boundary condition (1-η) g^i + η g^{i+1};
   c) compute J^1(T,g) with the new temperature;
   d) if J^1(T,g) < J(T,g) go to step 3, if J^1(T,g) > J(T,g) then compute η=0.5 η and go to step (a), if J^1(T,g) ≈ J(T,g) convergence is reached.

This algorithm can reduce strongly solution oscillations and therefore will be used in the numerical results section.

III. Numerical Results

In this section we report the numerical results of three smoothness controls obtained by using different values of the parameters β and λ. We consider three test problem cases: a simple problem with a standard boundary layer plane flow, a two and three-dimensional geometry with secondary flow injections at different temperatures. The objective functional in all cases is a desired constant temperature to be obtained in a specific region with support Ω_d where the weight function w(x) is defined.

For the numerical implementation of the different approaches and for the solution of the Navier-Stokes system we have used a finite-element multi-physics code with a multi-grid solver implemented. The coupled solution is obtained with standard GMRES solvers implemented by using the PETSC library. For large optimality system one may use Vanka solvers where the coupled optimality system is solved over a series of small subdomains [20]. The convergence of the solution is checked by its L^2 norm which takes into account the last two finest resolutions. Let M_{h1} be the coarser mesh and M_{h2} the refined mesh over the domain Ω and T_{h1} and T_{h2} the corresponding solutions. The convergence criteria is

$$\frac{\|T_{h1} - T_{h2}\|_{L^2(\Omega)}}{\|T_{h2}\|_{L^2(\Omega)}} < 10^{-4} \tag{17}$$

In all the tests the inequality (17) has been assumed to define the convergent solutions. In the rest of the paper the temperature and velocity fields and the physical properties are reported in non-dimensional values.

A. Boundary layer flow

In this paragraph we analyze the behavior of different solvers in a simple laminar fully developed plane flow. We define the inlet on the left side, the outlet on the right side, a symmetry plane on the top and the wall with the controlled temperature on the bottom, as reported in Fig. 1.

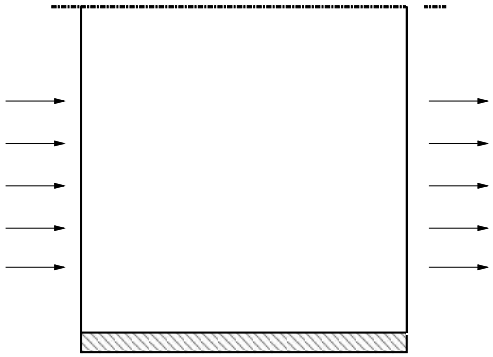

Figure 1. The plane boundary layer geometry. On the left inlet of the flow, on top symmetry axis, on bottom solid wall and on the right outlet.

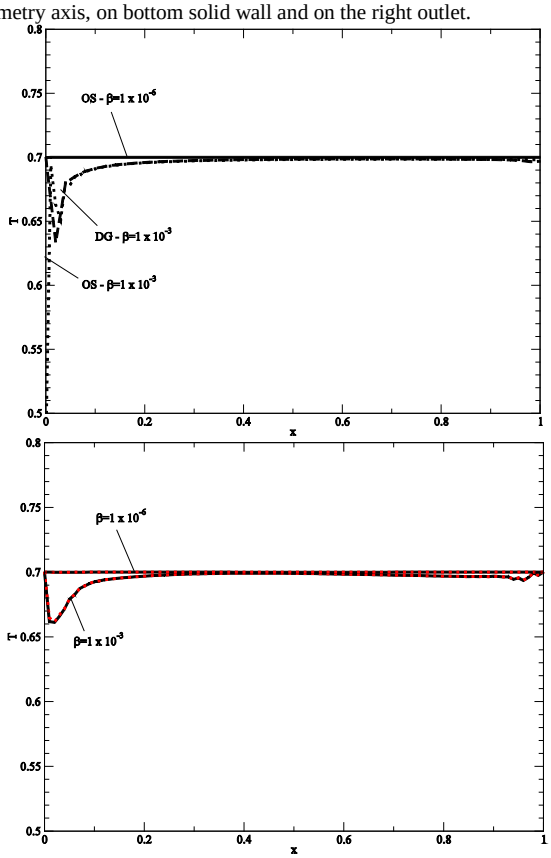

Figure 2. Plane boundary layer with T_d=0.7, temperature on the wall. One-shot case with quadratic elements (OS) and Discontinuous Galerkin method (DG) (top) and $\lambda \neq 0$ case (bottom). In the last graph dotted lines are for $\lambda = 10^{-6}$ while continuous for $\lambda = 10^{-3}$.

Two test cases have been studied with a different T_d. For the first test case the weight function is set to be w(x) = 1 along the whole domain and we seek for an analytical solution: we impose a non-dimensional inlet temperature of 0.7 and we set T_d = 0.7. The three approaches give different solution results, as we can see in Fig. 2. In this figure the temperature profile on the controlled wall is reported as a function of the axial coordinate x for the three approaches and different values of the parameters β and λ. In the graph on the left two temperature profiles for $\beta = 10^{-3}$ (dotted line) and $\beta = 10^{-6}$ (straight line) are reported as obtained with the first solution case. It is visible that the controlling parameter β has a great importance to obtain the correct solution. With the Discontinuous Galerkin method there are convergence problem to impose $\beta = 10^{-6}$ due to numerical errors. When β

TABLE 1

Solution Approach	J'
One-shot $\beta = 10^{-3}$	2.23×10^{-6}
One-shot $\beta = 10^{-6}$	3.40×10^{-12}
Discontinous Galerkin $\beta = 10^{-3}$	1.63×10^{-6}
$\beta = 10^{-3}$ and $\lambda = 10^{-3}$	1.48×10^{-6}
$\beta = 10^{-3}$ and $\lambda = 10^{-6}$	1.46×10^{-6}
$\beta = 10^{-6}$ and $\lambda = 10^{-3}$	2.68×10^{-12}
$\beta = 10^{-6}$ and $\lambda = 10^{-6}$	2.57×10^{-12}

Plane boundary layer with T_d=0.7, objective functional computed with different solution approaches.

tends to zero the control is not a standard function anymore and becomes a distribution and therefore it is not numerical representable in this approach. The result reported is the one with $\beta = 10^{-3}$ (dashed line). On the right we can see the results obtained by imposing $\lambda \neq 0$ and solving the control equation for g. By changing the parameter β one can obtain the correct solution, while by changing λ no relevant differences can be seen.

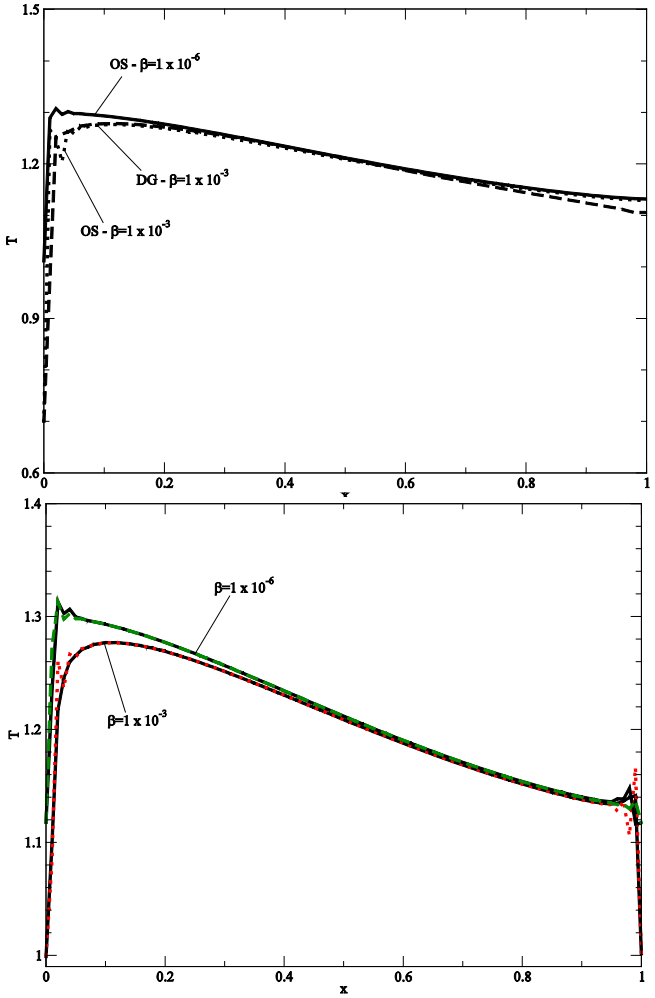

Figure 3. Plane boundary layer with T_d=1, temperature on the wall. One-shot case with quadratic elements (OS) with $\beta = 10^{-3}$ (dotted), 10^{-6} (continuous) and Discontinuous Galerkin method (DG) with $\beta = 10^{-3}$ (dashed) on top. Segregated approach with $\lambda = 10^{-3}$ (continuous line), $\beta = 10^{-3}$ and $\lambda = 10^{-6}$ (dotted), $\beta = 10^{-6}$ and $\lambda = 10^{-6}$ (dashed) on the bottom.

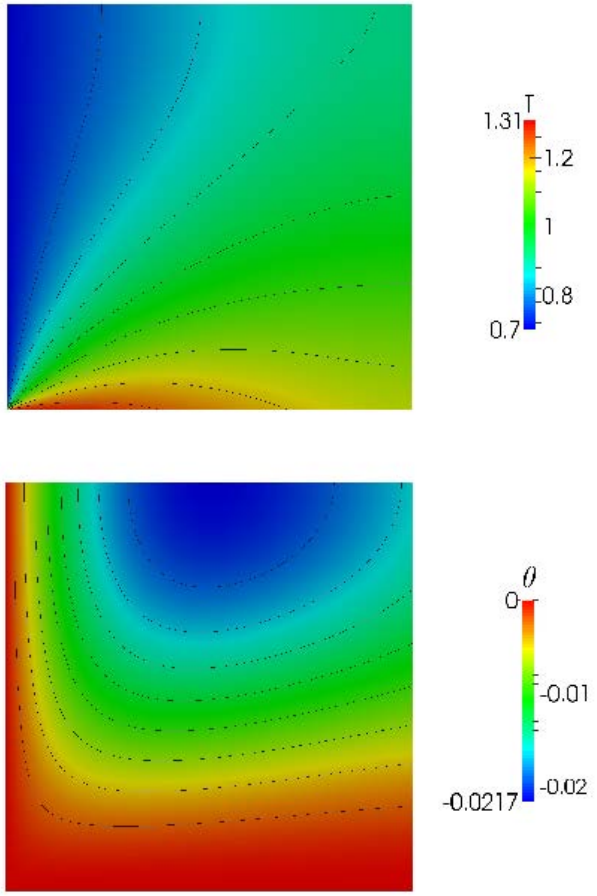

Figure 4. Plane boundary layer with Td=1, one-shot case with $\beta = 10^{-6}$. Temperature (top) and adjoint variable θ (bottom) contours obtained with ten equal subdivisions of the variable range.

In Table 1 the objective functional J' defined as $J' = 0.5 \int_{\Omega} (T(x) - T_d)^2 \, w(x) d\Omega$ is reported for different solution approaches. It can be clearly seen that the most powerful control is achieved by setting $\beta = 10^{-6}$ and that the best result for this case is obtained with the segregated approach with $\lambda = 10^{-6}$. It must be taken into account that this method is much slower than the one-shot method in obtaining a convergent solution.

In the other set of test cases which is studied with this geometry we still set the weight function w(x) = 1 but impose $T_d = 1$. We report the controlled solution and also some results for the adjoint temperature. In Fig. 3 we show the profile of the temperature on the controlled wall as computed in all the three cases. On the left the temperature profile is obtained with one-shot approach and Discontinuous Galerkin method while on the right with the segregated solver and g as additional variable. One-shot and DG methods give quite similar results for the temperature profile: the controlled wall tends to increase temperature of the fluid near the inlet while the temperature falls to 1.1 close to the outlet. The third approach shows ripples for cases with $\lambda = 10^{-6}$ and the profiles are different from the ones obtained with the other two approaches because near the outlet the temperature rises again. In Fig. 4

TABLE 2

Solution Approach	J'
One-shot $\beta = 10^{-3}$	1.0941×10^{-2}
One-shot $\beta = 10^{-6}$	1.0936×10^{-2}
Discontinous Galerkin $\beta = 10^{-3}$	1.0921×10^{-2}
$\beta = 10^{-3}$ and $\lambda = 10^{-3}$	1.0940×10^{-2}
$\beta = 10^{-3}$ and $\lambda = 10^{-6}$	1.0940×10^{-2}
$\beta = 10^{-6}$ and $\lambda = 10^{-3}$	1.0936×10^{-2}
$\beta = 10^{-6}$ and $\lambda = 10^{-6}$	1.0936×10^{-2}

Plane boundary layer with T_d=1, objective functional computed with different solution approaches.

the temperature and adjoint variable are reported for the one-shot case with $\beta = 10^{-6}$. Near the axis of symmetry, very far from the wall, the control cannot be enforced and the maximum absolute value of θ is reached. On the other side, near the wall the control is very good and the adjoint variable vanishes in this region.

Finally in Table 2 we report the values of the functional J' for this test case. We remark that the functional is several orders of magnitude higher than in the previous test case. We can see also that the parameter β is less important for this range of values and the lowest objective functional is achieved with the Discontinuous Galerkin method.

B. Two-dimensional mixing channel

In this paragraph we report the numerical results obtained in a more complex geometry in order to show the capability of the optimality system in real applications. We simulate a mixing channel in which a main flow mixes with another flow injected from a side of the channel with different temperature. The objective of the problem is to obtain a desired temperature in the flow lower than the inlet one but still higher than the walls. Moreover we decide to assign great importance to the center of the channel near the outlet by using the weight function $w(x) = 0.25 \, (8x\text{-}x^2) \, (y\text{-}y^2)$.

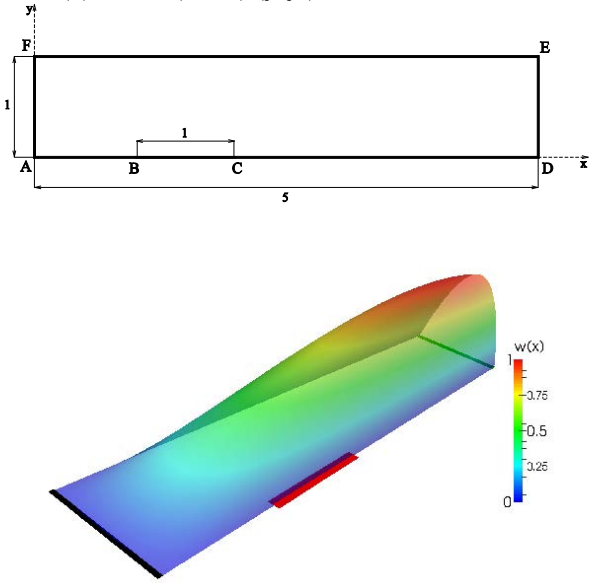

Figure 5. Mixing channel geometry (top) and weight function w(x) (bottom). The segment AF is the main flow inlet, BC is the secondary flow inlet, DE is the outflow.

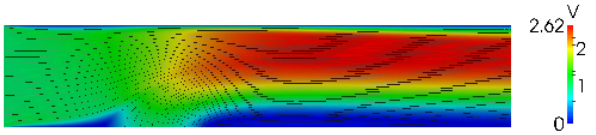

Figure 6. Velocity streamlines and velocity magnitude in the mixing channel.

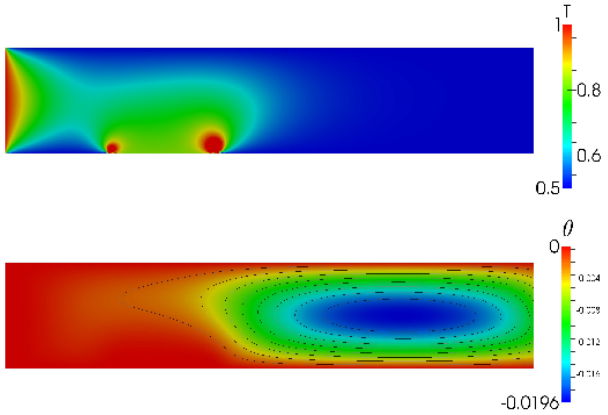

Figure 7. Temperature (top) and adjoint variable (bottom) computed with first approach and $\beta = 10^{-6}$.

In Fig. 5 the geometry and the weight function are reported over the computational domain. In this Figure the key regions are marked as follows: the segment AF is the inlet of the main flow, BC is the injection of the secondary flow with the controlled temperature and DE is the outlet. The other boundaries are solid walls with constant temperature.

As we have mentioned above we use a finite element solver for the solution of Navier-Stokes incompressible system to obtain the velocity field before solving the optimality system. We use Taylor-Hood finite elements with the same multi-grid solver of the optimality system for the solution of the Navier-Stokes equation. In Fig. 6 the velocity field is reported with flow streamlines and in colors the velocity magnitude. The injection flow is visible and a recirculation zone appears just after the injection region. With this velocity field we can solve the optimality system with different approaches as described before.

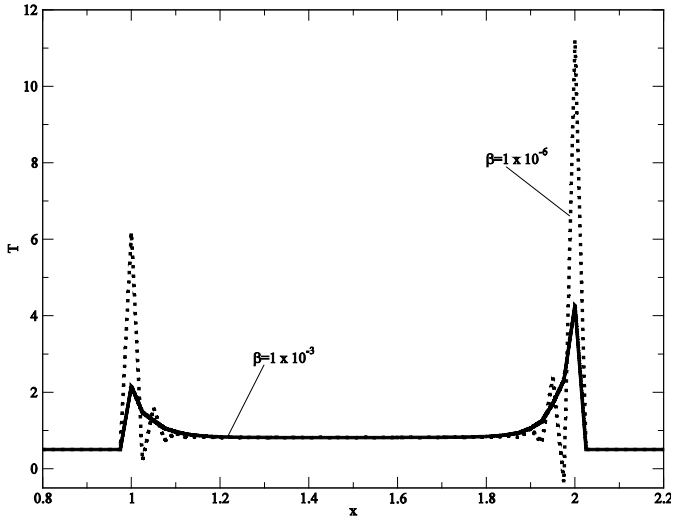

Figure 8. Temperature on the inlet line computed in the first case for $\beta = 10^{-3}$(continuous line) and $\beta = 10^{-6}$(dotted line).

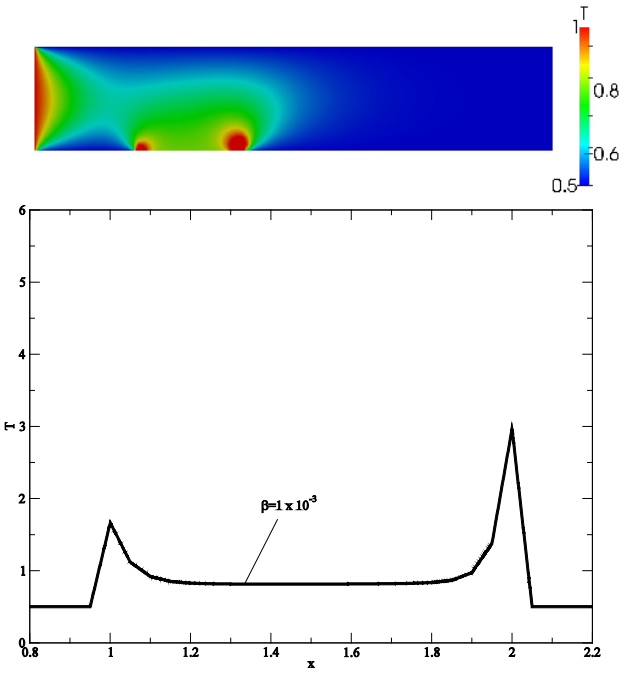

Figure 9. Temperature distribution on the whole domain (top) and on the inlet line (bottom) computed with Discontinuous Galerkin method and $\beta = 10^{-3}$.

The one-shot approach with quadratic elements shows to be very robust and the fully coupled solution with this approach is quite fast to obtain. The temperature and the adjoint variable fields, as obtained with the one-shot approach, are reported in Fig. 7 for $\beta = 10^{-6}$. We can see, as expected, that the region with high values of the adjoint variable is the region marked with the w(x) weight function. Having $\beta = 10^{-6}$ we can have a stronger control but the smoothness of the temperature on the controlled boundary decreases, as it can be seen in Fig. 8. The temperature is reported on the injection inlet line with coordinate x in the range of 0.8 to 2.2 for two values of $\beta = 10^{-3}$ and $\beta = 10^{-6}$. Strong oscillations of the temperature start to appear as the parameter β decreases under a certain value. On the contrary, with $\beta = 10^{-3}$,

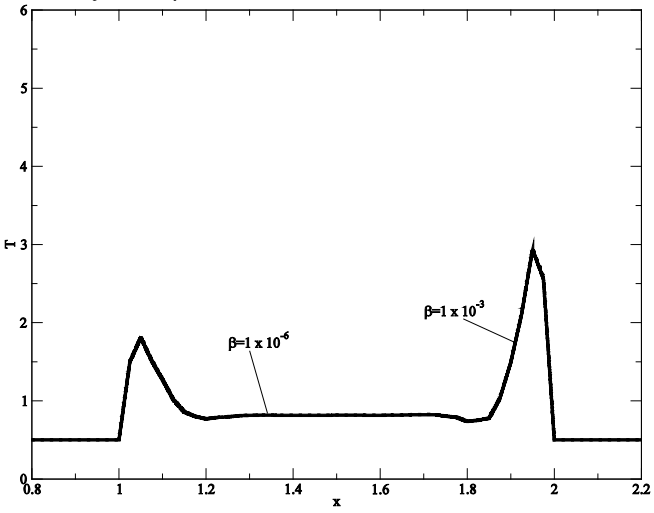

Figure 10. Temperature on the inlet line computed with third approach and $\beta = 10^{-3}$(continuous) and $\beta = 10^{-6}$(dotted), $\lambda = 10^{-3}$ in both cases.

TABLE 3

Solution Approach	J'
One-shot $\beta = 10^{-3}$	3.3039×10^{-2}
One-shot $\beta = 10^{-6}$	3.2960×10^{-2}
Discontinous Galerkin $\beta = 10^{-3}$	3.2890×10^{-2}
$\beta = 10^{-3}$ and $\lambda = 10^{-3}$	3.3275×10^{-2}
$\beta = 10^{-6}$ and $\lambda = 10^{-3}$	3.3270×10^{-2}

Two-dimensional mixing channel. Objective functional computed with different solution approaches and β-λ values.

the temperature is quite smooth but it has a sharp peak near the walls, where the inlet velocity v→0. The temperature distribution along the central region of the inlet flow is very similar for all different values of β.

The results obtained with the Discontinuous Galerkin method are reported in Fig. 9. On the left the temperature field is reported on the whole domain as computed with $\beta = 10^{-3}$ while on the right the temperature on the controlled inlet is shown as a function of the coordinate x in the range of 0.8 to 2.2. The result is quite similar to the one obtained with first approach showing sharp edges near the inlet wall and a flat non-dimensional temperature of around 0.8 in the center of the flow.

In Fig. 10 we report the temperature profile on the inlet line as computed with the third approach solving directly a differential equation for g. We consider solutions with $\lambda = 10^{-3}$ and with $\beta = 10^{-3}$ and 10^{-6}. In this figure two plots are reported with a straight continuous line for $\beta = 10^{-3}$ and with a dotted line for $\beta = 10^{-6}$. This profile shows similar peaks near the inlet walls as those obtained in the other two cases. It is important to remark some differences in the decreasing profile of the temperature near the peaks.

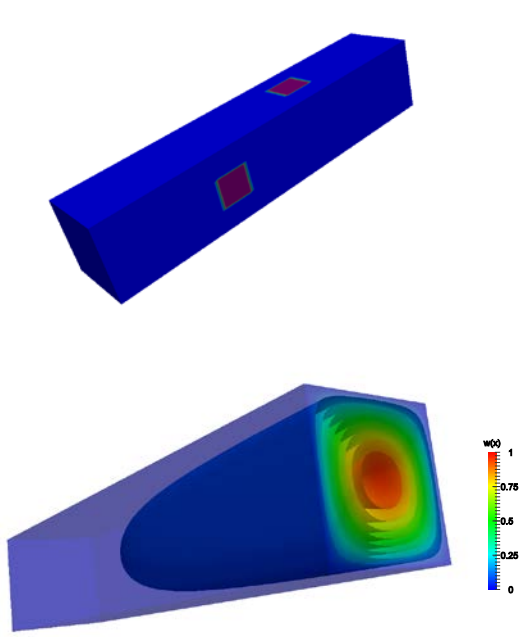

Figure 11. Three-dimensional mixing channel geometry with a scale factor of 0.1 in the axial direction (top), weight function on the same geometry (bottom). On the left the two flow injections are visible in red color and on the right ten equally subdivided isosurfaces for the weight function are reported. The flow is directed from left to right in both figures.

Finally we can compute the objective functional J' and compare the results. In Table 3 the functional is reported for the injection test case and for all the different cases and β values employed. As already remarked, from this table one can see that by imposing a lower value of β the control is more effective. All the methods give quite similar values but the best result is obtained with the Discontinuous Galerkin method. The solution obtained with the segregated method is smoother and therefore the control loses effectiveness. For this reason it gives the worst results in term of functional J'. The one-shot approach with quadratic elements lies between the other two. The result that gives high temperature oscillations near the wall corresponds to a low functional value.

C. *Three-dimensional mixing channel*

In this paragraph we report the numerical results obtained in a three-dimensional test case. The geometry is a channel with a main flow entering from the bottom and two injections of a fluid with controlled temperature on two sides. The axial domain dimension is 5 while the other two dimensions x and y are 0.1. The injections are located between z = 1.5-2 and z=3-3.5 and are 0.05 wide. A three-dimensional view of the geometry is reported in Fig. 11 with a scale factor of 0.1 in the axial direction. In this Figure the injections are reported in red color while the walls are blue. The main inlet velocity is 2 while the secondary injection velocities are 0.5 in the normal direction of the inlet.

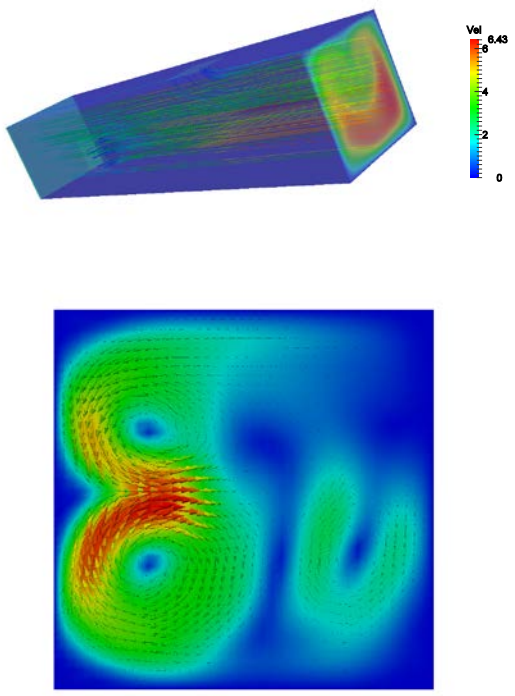

Figure 12. Velocity flow pattern of the three-dimensional mixing channel geometry. Velocity streamlines colored by the velocity magnitude (top) and

velocity on a slice obtained at a constant axial coordinate z=4 with arrows colored by velocity magnitude (bottom).

The main inlet temperature and the wall temperature are assigned as 0.5, while the temperature of the two injection flows is controlled. The control objective is to obtain a constant temperature near the outlet of the channel and this can be accomplished with a weight function as

$$w(x) = (0.12z^2 - 0.016z^3)\left(e^{\frac{\ln(2)z}{5}} - 1\right)(40y - 400y^2)(40x - 400x^2)$$

This weight function is reported in Fig. 11 with a geometrical scale factor of 0.1 in the axial direction and with ten equally spaced isosurfaces of the weight function in the range of 0 to 1.

The velocity field of the incompressible Navier-Stokes system can be solved separately from the optimality system, as explained before. The solution of the velocity and pressure fields requires high computational cost because of the three-dimensional problem. On the left of Fig. 12, the flow pattern is visible with the velocity streamlines reported on the three-dimensional domain and colored by the velocity magnitude. One can see the formation of vortices due to the lateral injections. A slice obtained at axial coordinate z = 4 is reported in Fig. 12 on the right with the velocity vectors represented with arrows and colored by the velocity magnitude. The recirculation patterns are visible in this Figure and the flow on the outlet section is pushed towards a corner of the channel by two recirculation vortices.

For this test case the optimality system has been solved with the one-shot approach because of its robustness and fast convergence obtained in the other test cases. The temperature results obtained with β = 0.1 are reported in Fig. 13. In this Figure the temperature is shown with ten equally subdivided isosurfaces on the domain clipped with a section normal to the

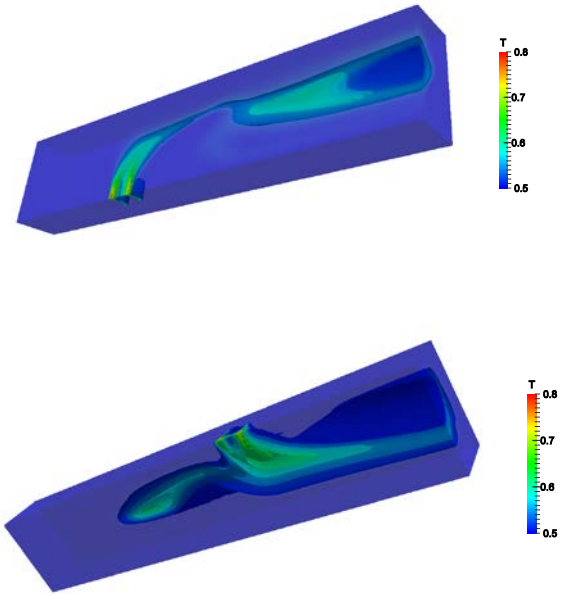

Figure 13. Temperature profile obtained with β=0.1 in the three-dimensional mixing channel geometry. Ten equally spaced temperature isosurfaces on half of the domain clipped with a section normal to the x-axis (top) and section normal to the y-axis (bottom).

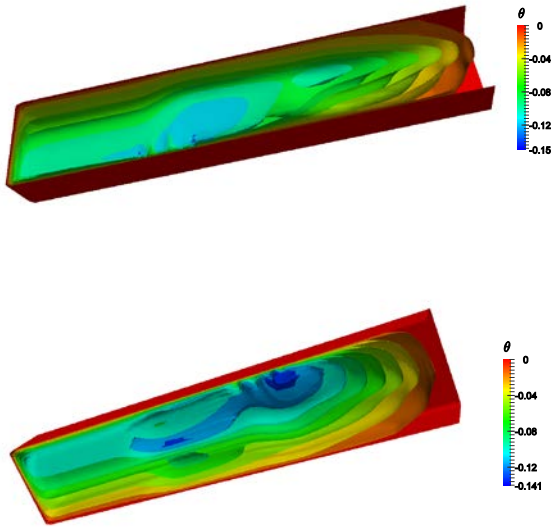

Figure 14. Adjoint variable profile obtained with β=0.1 in the three-dimensional mixing channel geometry. Ten equally spaced temperature isosurfaces on half of the domain clipped with a section normal to the x-axis (top) and section normal to the y-axis (bottom).

x-axis on the left and y-axis on the right. On the left, one can see the effect of the first injection located between z = 1.5-2 and on the right it can be seen the second injection located between z = 3-3.5. The control on the boundary tries to heat the flow by increasing temperature on the two injections. The hottest fluid moves along the channel achieving a lower functional J'. It is interesting to study also the adjoint variable in order to better understand the control problem.

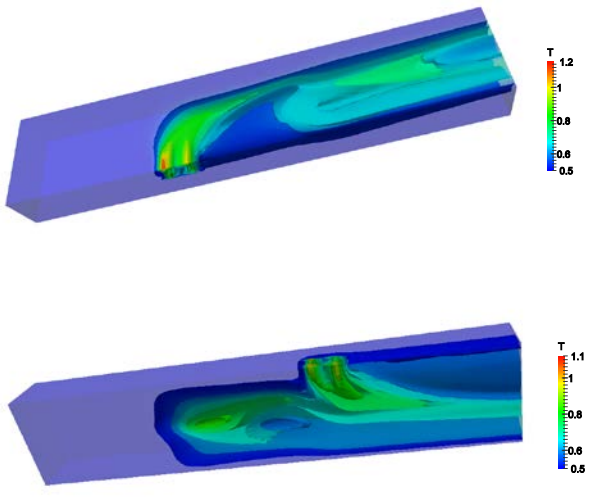

Figure 15. Temperature profile obtained with β=0.05 in the three-dimensional mixing channel geometry. Ten equally spaced temperature isosurfaces on half

of the domain clipped with a section normal to the x-axis (top) and section normal to the y-axis (bottom).

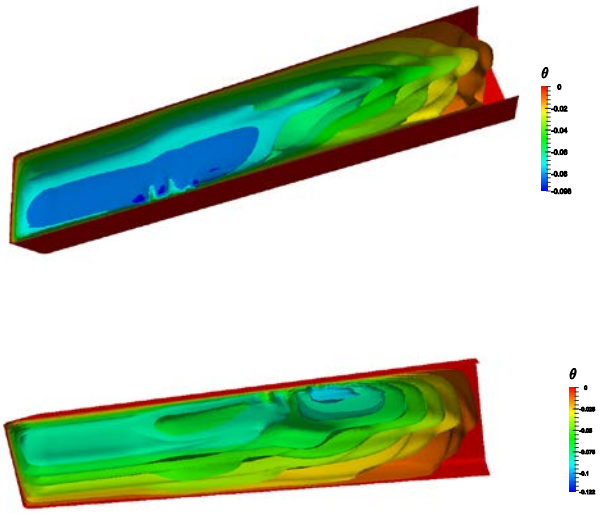

Figure 16. Adjoint variable profile obtained with β=0.05 in the three-dimensional mixing channel geometry. Ten equally spaced temperature isosurfaces on half of the domain clipped with a section normal to the x-axis (top) and section normal to the y-axis (bottom).

In Fig. 14 the adjoint variable is reported with ten equally subdivided isosurfaces. On the left the domain is clipped with a plane normal to the x-axis, on the right with respect to y-axis. The adjoint or importance function is higher in modulus where the control should act stronger in order to better achieve the desired result. In this problem the velocity is quite high and the adjoint variable is higher towards the inlet of the channel since changing the temperature in this region would control better the result. A possible way of taking into account this information could be to set the injections upstream in the axial direction.

By decreasing the parameter β to 0.05 the control acts stronger to decrease the objective functional because the solution T on the boundary can take higher values. In Fig. 15 the temperature is reported with ten equally subdivided isosurfaces on the domain clipped with respect to the x (left) and y-axis (right). It can be seen from this Figure that the values attained by the temperature on the controlled surfaces are higher in modulus than the ones obtained by setting β=0.1. The adjoint variable for this case is reported in Fig. 16 and it is shown with ten equally subdivided isosurfaces. On the left the domain is clipped with respect to the x-axis and on the right with respect to the y-axis. By decreasing β the adjoint variable becomes lower and the region where the control cannot reduce the objective functional is more visible.

We can now compare the temperature distributions obtained on the outlet section for two different values of β. On the left of Fig. 17 the results of the test case with β = 0.1 is reported, while on the right those with β = 0.05. Over this section the vortices created by the flow are well visible. Moreover we remark the different ranges of temperature with the different β, with the maximum temperature obtained for β = 0.05. Finally in Table 4 we compare the objective functional obtained with the one-shot approach and β = 0.1, 0.05. It is clear the

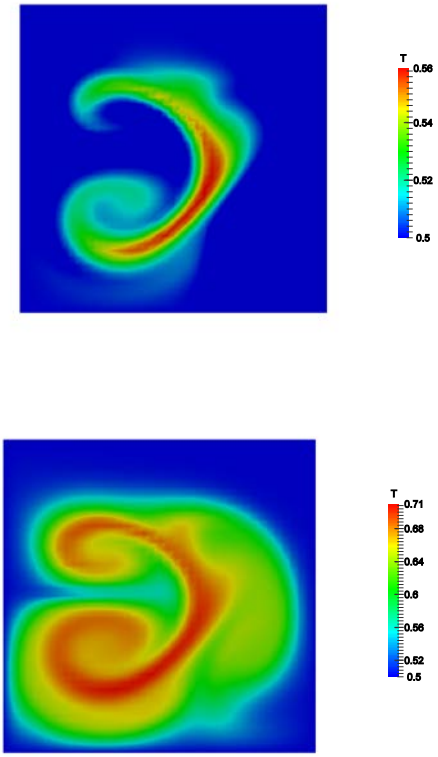

Figure 17. Temperature distribution on the outlet section of the three-dimensional mixing channel. Test case with β=0.1 (top) and β=0.05 (bottom).

TABLE 4

Solution Approach	J'
One-shot $\beta = 0.1$	1.722×10^{-3}
One-shot $\beta = 0.05$	1.054×10^{-3}

Three-dimensional mixing channel test case, objective functional computed with different β values.

important effect of the regularization parameter β in achieving low functional values.

IV. Conclusion

In this paper the optimal boundary control problem for the energy equation driven by Navier-Stokes incompressible flow has been analyzed. We have proposed and compared three different approaches to the solution of the optimality system. An extrapolated way of setting Dirichlet boundary condition for the controlled temperature in the one-shot approach with standard finite elements has been proposed. We have reported numerical results obtained in two and three-dimensional geometries with different values of the optimality system parameters.

We have found that the integral boundary condition, for the controlled temperature setting, gives a very high stability to the fully coupled solution even with very low values of β. The parameter β, as defined in equation (1), has a strong influence

in control effectiveness, while the parameter λ is important only for increasing the controlled temperature smoothness. The fully coupled one-shot approach has shown the best convergence properties although not always the best solution in term of smoothness and objective functional. The Discontinuous Galerkin method gives very good results because in many test cases it allows to compute the lowest objective functional, but it has some convergence issues. The last approach with segregated solution and an additional transport equation for the control is much more suitable for searching smoother profiles. The solution algorithm is quite slow and some improvements are necessary. The results obtained with this approach are however quite good and, as expected, the temperature profiles are smoother than the ones obtained with all the other approaches.

REFERENCES

[1] M.D. Gunzburger, *Perspectives in Flow Control and Optimization*, Advances in Design and Control, SIAM, 2003.

[2] Karlheinz Spindler, *Optimal Control on Lie Groups: Theory and Applications*, Wseas Transactions on Mathematics, Issue 5, vol. 12, pp. 531-542, 2013.

[3] K. Ito, S.S. Ravindran, *Optimal control of thermally convected fluid flows*, SIAM Journal on Scientific Computing, vol. 19 (6), pp. 1847-1869, 1998.

[4] K.W. Morton, *Numerical Solution of Convection-Diffusion Problems*, Chapman & Hall, London, Glasgow, New York, 1996.

[5] R.A. Bartlett, M. Heinkenschloss, D. Ridzal and B.G. Waanders, *Domain decomposition methods for advection dominated linear-quadratic elliptic optimal control problems*, Computer Methods in Applied Mechanics and Engineering, vol. 195, pp. 6428-6447, 2006.

[6] N.M. Arifin and N.H. Abidin, *Marangoni Convection in a Variable Viscosity Fluid Layer with Feedback Control*, Wseas Transactions on Mathematics, vol. 8 (8), pp. 373-382, 2009.

[7] M. Gunzburger and S. Manservisi, *Analysis and approximation of the velocity tracking problem for Navier-Stokes flows with distributed control*, SIAM Journal of Numerical Analysis, vol. 37 (5), pp. 1481-1512, 2000.

[8] M. Gunzburger, H. Kim and S. Manservisi, *On a shape control problem for the stationary Navier-Stokes equations*, ESAIM Mathematical Modelling and Numerical Analysis, vol. 34 (6), pp. 1233-1258, 2000.

[9] Sandro Manservisi, *An extended domain method for optimal boundary control for Navier-Stokes equations*, International Journal of numerical analysis and modeling, vol. 4 (3), pp. 584-607, 2007.

[10] H. Lee and O. Imanuvilov, *Analysis of Neumann boundary optimal control problems for the stationary Boussinesq equations including solid media*, SIAM Journal on Control and Optimization, vol. 39 (2), pp. 457-477, 2000.

[11] G. Bornia, M.D. Gunzburger and S. Manservisi, *A distributed control approach for the boundary optimal control of the steady MHD equations*, Communications In Computational Physics, vol. 14 (3), pp. 722-752, 2013.

[12] M. Gunzburger and S. Manservisi, *The velocity tracking problem for Navier-Stokes flow with boundary control*, SIAM Journal on Control and Optimization, vol. 39 (2), pp. 594-634, 2000.

[13] H.M. Park and W.J. Lee, *Feedback control of natural convection*, Computer Methods in Applied Mechanics and Engineering, vol. 191 (8-10), pp. 1013-1028, 2001.

[14] M.D. Gunzburger and S. Manservisi, *The velocity tracking problem for Navier-Stokes flow with linear feedback control*, Journal of Computer Methods in Applied Mechanics and Engineering, vol. 189 (3), pp. 803-823, 2000.

[15] Subhransu Padhee, *Controller Design for Temperature Control of Heat Exchanger System: Simulation Studies*, Wseas Transactions on Systems and Control, vol. 9, pp. 485-491, 2014.

[16] D.N. Arnold, F. Brezzi, B. Cockburn and L.D. Marini, *Unified analysis of discontinuous Galerkin methods for elliptic problems*, SIAM Journal on Numerical Analysis, vol. 39 (5), pp. 1749-1779, 2002.

[17] B. Cockburn, G.E. Karniadakis, C.W. Shu, *Discontinuous Galerkin Methods:Theory, Computation and Applications*, Series: Lecture Notes in Computational Science and Engineering, Springer, vol. 11, 2000.

[18] R. Adams, *Sobolev Spaces*, Academic Press, New York, 1975.

[19] S.C. Brenner and L.R. Scott, *The mathematical theory of finite element methods*, Springer-Verlag, 2002.

[20] S. Manservisi, *Numerical analysis of Vanka-type solvers for steady Stokes and Navier-Stokes flows*, SIAM Journal on Numerical Analysis, vol. 44 (5), pp. 2025-2056, 2006.